Russian Chemical Reviews **79** (1) 1 – 11 (2010) © 2010 Russian Academy of Sciences and Turpion Ltd

DOI 10.1070/RC2010v079n01ABEH004088

New superconductors based on five-component transition metal oxypnictides

A L Ivanovskii

Contents

I.	Introduction	1
II.	The synthesis of 32225 and 42226 phases	2
III.	Crystal structure and properties	3
IV.	Simulation of the electronic structures of 32225 and 42226 phases	6
V.	Conclusion	10

Abstract. A review of layered five-component transition metal oxypnictides ($Sr_3Sc_2Fe_2As_2O_5$, $Sr_4V_2Fe_2As_2O_6$, $Sr_4Sc_2Fe_2P_2O_6$, *etc*.) discovered recently is presented. They constitute a new family of the so-called 32225 and 42226 phases, which are promising materials for the quest for high-temperature superconductors. The methods of synthesis, features of crystal structures, physicochemical properties as well as models of electronic structure and chemical bonding for these phases are discussed. The bibliography includes 63 references.

I. Introduction

One of the most significant discoveries of 2008 in the physicochemistry of superconducting materials was the detection [1] of a transition of the oxyarsenide doped with flouride ions $LaFeAsO_{1-x}F_x$ to the superconducting state (a critical transition temperature is $\sim$26 K). This discovery initiated a subsequent intensive quest for related superconducting compounds. Over the past period, numerous so-called FeAs-superconductors have been synthesized and investigated. They are represented by the following major groups:[2–5]

— oxygen-containing 1111 phases based on layered (structural type ZrCuSiAs, space group *P*4/*nmm*) four-component oxyarsenides LnFeAsO (Ln = La, Ce, ... Gd, Tb, Dy); this group includes the above-mentioned oxyarsenide $LaFeAsO_{1-x}F_x$;

— isostructural oxygen-free 1111 phases based on four-component fluoroarsenides AFeAsF (A = Sr, Ca, Eu);

— three-component layered (structural type $ThCr_2Si_2$, space group *I*4/*mmm*) superconductors based on AFe_2As_2 (A = Sr, Ba), 122 phases;

— three-component layered (space group *P*4/*nmm*) superconductors based on LiFeAs and NaFeAs, 111 phases.

Let us highlight the most essential features of these materials.[2–5] All the FeAs-based superconductors are anisotropic (quasi-two-dimensional) systems, their crystal structures include the negatively charged $[Fe_2As_2]^{\delta-}$ blocks alternating with either the positively charged $[LnO]^{\delta+}$, $[AF]^{\delta+}$ layers (for 1111 phases) or planar networks of alkali or alkaline-earth metal ions (for 122 or 111 phases), respectively. Superconductivity of all these compounds is associated with the state of the $[Fe_2As_2]$ blocks, which make a determining contribution to the density of states near the Fermi level of these materials, whereas $[LnO]^{\delta+}$, $[AF]^{\delta+}$ layers that separare them or networks of alkali or alkaline-earth metal ions serve as so-called charge reservoir layers. A number of other features of FeAs-superconductors are noted in the reviews. [2–5]

An interesting correlation between the spacing between the conducting $[Fe_2As_2]$ blocks incorporated into FeAs-superconductors and their critical temperature values T_c was revealed.[6] Thus the maximum values of T_c ($\sim$55–57 K) were reached for a number of doped 1111 phases [7,8] in the structures of which the distances (L) between neighbouring blocks $[Fe_2As_2]/[Fe_2As_2]$ separated by the $[LnO]^{\delta+}$ or $[AF]^{\delta+}$ blocks are $\sim$8.7 Å. For 122 phases where the $[Fe_2As_2]/[Fe_2As_2]$ neighbouring blocks are separated by monoatomic networks of alkaline-earth metals ($L \approx 6.5$ Å), T_c values are appreciably lower, down to 38 K.[9–11] Even lower critical temperatures ($\sim$18 K) were detected,[12,13] for 111 phases in which the $[Fe_2As_2]/[Fe_2As_2]$ blocks are separated by alkali metal networks ($L \approx 6.4$ Å). In the same series it is appropriate to mention related iron-containing Fe–Se-superconductors with tetragonal structure (the type is anti-PbO, the space group is *P*4/*nmm*) and the directly contacting layers $[Fe_2Se_2]/[Fe_2Se_2]$ for which T_c does not exceed 7–8 K under usual conditions.[14]

The nature of such a correlation is not clear so far. One of possible explanations [6] rests on the hypothesis about an important role of spin fluctuations in the superconductivity mechanism of FeAs-materials. According to this hypothesis, an increase in the distance between superconducting

A L Ivanovskii Institute of Solid State Chemistry, Ural Branch of the Russian Academy of Sciences, ul. Pervomaiskaya 91, 620990 Ekaterinburg, Russian Federation. Fax (7-343) 374 44 95, tel. (7-343) 374 53 31, e-mail: ivanovskii@ihim.uran.ru

Received 17 July 2009
Uspekhi Khimii **79** (1) 3 – 14 (2010); translated by A F Nasonov

$[Fe_2As_2]/[Fe_2As_2]$ blocks should prevent the formation of a long-range antiferromagnetic order, which will favour the increase in T_c.

In this context, of significant interest is a new family of more complex five-component compounds that includes groups of 32225 and 42226 phases, which was discovered in early 2009.[6, 14–25] Their prototypes were $Sr_3Sc_2Fe_2As_2O_5$ for 32225 phases (Ref. 6), $Sr_4Sc_2Fe_2P_2O_6$ (Ref. 22) and $Sr_4Sc_2Fe_2As_2O_6$ (Ref. 17) for 42226 phases. The most important features of the family of 32225 and 42226 phases that distinguish them from the above-mentioned groups of superconducting FeAs-materials are the following.[6, 15–25]

Like the groups of 1111, 122, and 111 phases, 32225 and 42226 phases comprise $[Fe_2As_2]$ blocks. However, these blocks in the structures of the latter are at extremely large distances from each other: $L \approx 13.4$ Å (for 32225 phases) and $L \approx 15.5$ Å (for 42226 phases).

In the structure of 32225 and 42226 phases, the $[Sr_3M_2O_5]$ or $[Sr_4M_2O_6]$ oxide blocks (charge reservoirs), which separate the neighbouring $[Fe_2As_2]/[Fe_2As_2]$ blocks, contain atoms of d-transition metals (M = Sc, Ti, V, Cr), while in 1111, 122 and 111 phases this role is played by the blocks (atomic networks) containing exlcusively alkali, alkaline-earth or rare-earth metals.[2–5]

For 1111 and 122 phases, the transition to the superconducting state is achieved through electron or hole doping by introducing alkaline-earth or rare-earth metals into charge reservoir blocks or d-metal impurities into the conducting $[Fe_2As_2]$ blocks.[2–5] For new 42226 phases, it was discovered that a transition to the superconducting state can be attained by doping the $[Sr_4M_2O_6]$ blocks with transition metal atoms, for example, upon partial substitution of titanium for scandium in $Sr_4Sc_2Fe_2As_2O_6$ or $Ca_4Sc_2Fe_2As_2O_6$ (Ref. 18) or titanium for chromium in $Sr_4Cr_2Fe_2As_2O_6$.[19]

By the example of the $Sr_4Mg_{1+x}Ti_{1-x}As_2O_6$ phase, yet another possibility of a wide variation in the critical temperature (from 10 to 39 K) upon partial replacement of the Ti^{4+} ions by the Mg^{2+} ions was detected.[25]

Finally, among 42226 phases a critical temperature of $\sim$17 K was registered for $Sr_4Sc_2Fe_2P_2O_6$. Currently, this is the maximum value among all the known T_c values for phosphorus-containing analogues of FeAs-superconductors.[22] For $Sr_4V_2Fe_2As_2O_6$, a transition to the superconducting state at $\sim$37 K was reported.[20] This is also a record value for all the known undoped FeAs-systems.

The present review surveys currently available data on the methods of synthesis, structures, properties as well as on the electronic structure simulation of a new family of 32225 and 42225 phases. The basic aim of this publication is an attempt to attract researchers' attention to this new family of layered five-component oxypnictide phases, which are promising for the search for novel FeAs-superconductors and the systems a detailed study of the properties of which should lead to a deeper understanding of the physicochemistry of the whole class of FeAs-superconductors.

II. The synthesis of 32225 and 42226 phases

In the pioneering work,[6] a two-step method of solid-phase synthesis was employed for the preparation of polycrystalline $Sr_3Sc_2Fe_2As_2O_5$. In the first step, precursors, the binary arsenides SrAs, ScAs, were obtained from elemental Sr, Sc and As, which further were used as reactants in the synthesis of the target product. For this purpose, they were mixed with Sc_2O_3, SrO, Fe_2O_3 and powdered iron in the ratio that corresponded to the $Sr_3Sc_2Fe_2As_2O_5$ stoichiometry. The mixture was pressed into pellets that were placed into a quartz tube. All the procedures were carried out in an inert

Table 1. The synthesis of FeAs-phases 32225 and 42226 and related five-component systems.

Synthesized phase	T_c /K	Solid-phase synthesis			Ref.
		reactants	T/°C	t/h	
$Sr_3Sc_2Fe_2As_2O_5$	–	$SrAs + ScAs + Sc_2O_3 + SrO + Fe_2O_3 + Fe$	1000	4	6
$Sr_3Sc_2Fe_2As_2O_5$	–	$Sc_2O_3 + SrO + FeO + As_2O_3$	1050	60	15
$Sr_3(Sc_{0.8}Ti_{1.2})Fe_2As_2O_5$	–	$SrAs + SrO + Sc_2O_3 + Fe + FeAs + Fe_2As + TiO_2$	1150	50	18
$Sr_4Sc_2Fe_2As_2O_6$	–	$SrAs + Fe_2As + SrO + Sc_2O_3$	900	10	16
$Sr_4Sc_2Fe_2As_2O_6$	–	$FeAs + SrO + Sr + Sc_2O_3$	1000	24	17
$Sr_4Sc_2Fe_2As_2O_6$	–	$SrAs + SrO + Sc_2O_3 + Fe + FeAs + Fe_2As$	1150	50	18
$Ba_4Sc_2Fe_2As_2O_6$	–	$Ba + Sc + Fe_2O_3 + As_2O_3$	1050	60	24
$Sr_4(Sc_{2-x}Ti_x)Fe_2As_2O_6$ ($x \approx 0-0.6$)	45 [a]	$SrAs + SrO + Sc_2O_3 + Fe + FeAs + Fe_2As + TiO_2$	1150	50	18
$Sr_4V_2Fe_2As_2O_6$	–	$V_2O_5 + SrO_2 + Sr + FeAs$	1150	36	21
$Sr_4V_2Fe_2As_2O_6$	37.2	$SrAs + V_2O_5 + SrO + Fe + Sr$	1150	40	20
$Sr_4Cr_2Fe_2As_2O_6$	–	$FeAs + SrO + Sr + Cr + Cr_2O_3$	1200	50	17
$Sr_4Cr_2Fe_2As_2O_6$	–	$Sr + Cr + Fe_2O_3 + As_2O_3$	1050	60	24
$Sr_4(Cr_{0.8}Ti_{1.2})Fe_2As_2O_6$	29.2 [a]	$SrAs + FeAs + Cr_2O_3 + SrO + TiO_2 + Ti + Fe$	1000	40	19
$Sr_4(Mg_{1+x}Ti_{1-x})Fe_2As_2O_6$	39	$FeAs + SrO + MgO + Ti + TiO_2$	1250	72	25
$Ca_4Sc_2Fe_2As_2O_6$	–	$CaAs + CaO + Sc_2O_3 + Fe + FeAs + Fe_2As$	1150	50	18
$Ca_4(Sc_{0.8}Ti_{1.2})Fe_2As_2O_6$	37 [a]	$CaAs + CaO + Sc_2O_3 + Fe + FeAs + Fe_2As + TiO_2$	1150	50	18
$Sr_4Sc_2Co_2As_2O_6$	–	$SrAs + Co_2As + SrO + Sc_2O_3$	1200	50	16
$Sr_4Sc_2Ni_2As_2O_6$	2.7	$SrO + Sr + Sc_2O_3 + NiAs$	1100 – 1200	16 – 48	23
$Sr_4Sc_2Fe_2P_2O_6$	17 [a]	$FeP + SrO + Sr + Sc_2O_3$	900 – 1200	40	22
$Sr_4Sc_2Ni_2P_2O_6$	3.3	$SrO + Sr + Sc_2O_3 + Ni + P$	1100 – 1200	18 – 48	23

[a] The temperature of the beginning of a transition to the superconducting state [$T_c^{(o)}$].

atmosphere. An annealing was performed at 1000 °C for 40 h.

The same phase was also synthesized by a somewhat different technique.[15] A mixture $Sc_2O_3 + SrO + FeO + As_2O_3$ was employed, which was placed in a quartz tube and sealed in a purified argon atmosphere. The tube was heated to 1050 °C at a rate of 200 deg h^{-1}, kept at this temperature for 60 h and then cooled to room temperature. The product was homogenized, pressed into pellets and reannealed at 1050 °C for 60 h.

For the synthesis of 42226 phases, a sufficiently large number of methods were proposed,[16–25] the main characteristics of them are presented in Table 1. As a rule, binary oxides or specially synthesized metal pnictides as well as powders of pure metals are utilized as reactants. The temperature of thermal treatment of a charge mixture (pellets) lies within the interval 900–1200 °C, the annealing time, as a rule, is several tens of hours.

It should be emphasized that all the currently obtained samples of 32225 and 42226 phases are polycrystalline, as distinct from, for instance, a number of 1111 and 122 FeAs-phases, which could be synthesized as single crystals.[3,5] In addition, in the samples of 32225 and 42226 phases, as a rule, there are secondary two- or three-component phases produced upon sintering the charge mixture, which can be detected in X-ray diffraction spectra. Thus ternary phosphide $SrFe_2P_2$ was discovered as the secondary phase in the manufacture of $Sr_4Sc_2Fe_2P_2O_6$, the ratio of phases $Sr_4Sc_2Fe_2P_2O_6 : SrFe_2P_2$ in the sample is estimated[22] as $\sim 9:1$. In the synthesis of $Sr_4V_2Fe_2As_2O_6$, for which, as noted above,[20] one of the highest critical temperature (~ 37 K) was reported for this family of phases, FeAs and Sr_2VO_4 were the secondary (impurity) phases.

Pay attention to yet another interesting fact. An attempt was made[18] to obtain the doped phase $Sr_4Sc_2Fe_2As_2O_6$ by partial replacement of Sc^{3+} by Ti^{4+}. To this end, a solid-phase synthesis was carried out from SrAs, SrO, Sc_2O_3, Fe, FeAs, Fe_2As and TiO_2 as the reactants mixed with account of the supposed stoichiometry of phases $Sr_4(Sc_{2-x}Ti_x)$-$Fe_2As_2O_6$ with a varying content of Sc and Ti. At small concentrations of titanium ($x < 0.6$), doped phases of the 42226 type (space group $P4/nmm$) were obtained, whereas at higher content of titanium, phases of the 32225 type (space group $I4/mmm$) were formed. Reasons for the stabilization of different phases (42226 or 32225) upon variation in the concentration of Sc and Ti have not been studied yet.

Finally, yet another important conclusion follows from Refs 15–25, *viz*., a significant chemical lability of oxide layers in 32225 and 42226 phases.

III. Crystal structure and properties

The discussed 32225 and 42226 phases have tetragonal structures. Note that a number of their isostructural analogues have been known earlier. Thus the mineral chalcothallite $(K/Tl)_2Cu_7SbS_4$ (Ref. 26) is the prototype of a group of 32225 phases, the same group includes the $Sr_3Fe_2Cu_2S_2O_5$, $Sr_3Sc_2Cu_2S_2O_5$ (Refs 27 and 28) phases and some others.[15] The five-component oxysulfide $Sr_4Ga_2Cu_2S_2O_6$ is mentioned[28] as the prototype of 42226 phases.

The structures of 32225 and 42226 phases are layered and composed (for example, in the case of $Sr_3Sc_2Fe_2As_2O_5$ and $Sr_4Sc_2Fe_2As_2O_6$) of the ...$[Fe_2As_2]$/$[Sr_3Sc_2O_5]$/$[Fe_2As_2]$... and ...$[Fe_2As_2]$/$[Sr_4Sc_2O_6]$/$[Fe_2As_2]$... layers

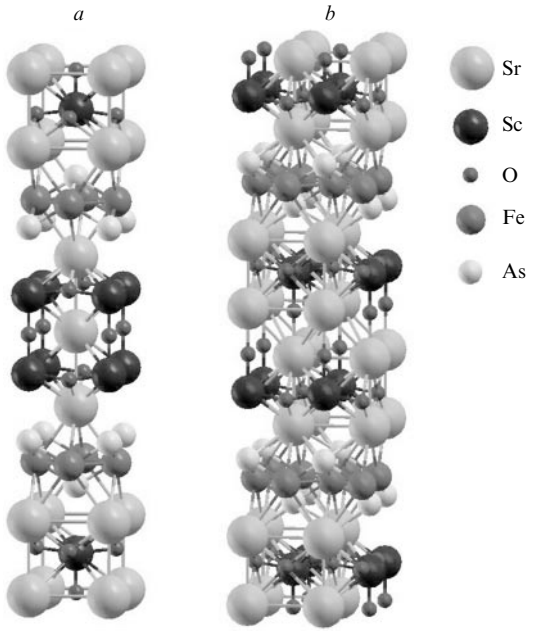


Figure 1. Fragments of the crystal structure of 32225 and 42226 phases by the example of $Sr_3Sc_2Fe_2As_2O_5$ (*a*) and $Sr_4Sc_2Fe_2As_2O_6$ (*b*).

(blocks) packed along the *c* axis (Figs 1 and 2). Hence, in the literature one can encounter a different designation of the chemical formulas of 32225 and 42226 phases, which takes into account the composition and alternation of accentuated structural blocks, for instance, $(Sr_3Sc_2O_5)$. $.Fe_2As_2$ and $(Sr_4Sc_2O_6)Fe_2As_2$ or $(Sr_2ScO_3)FeAs$.

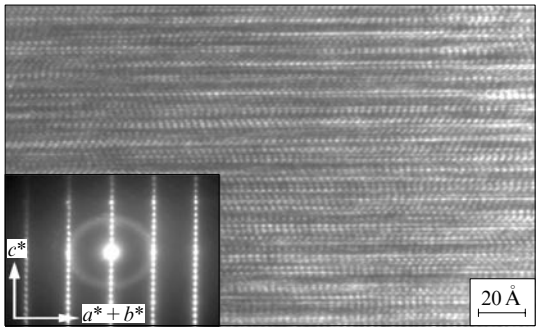


Figure 2. The atomic structure of $Sr_4Sc_2Fe_2As_2O_6$ according to transmission electron microscopy and electron diffraction (inset).[17]

For 32225 phases, the $[Fe_2As_2]$ blocks (as in 1111, 122 and 111 FeAs-phases)[2–5] consist of a network of iron atoms with arsenic atoms arranged above and below them. The coordination number of the iron atoms is 4, their coordination polyhedra are the $FeAs_4$ tetrahedra compressed along the *c* axis. In other words, the $[Fe_2As_2]$ blocks can be represented as the edge-sharing $FeAs_4$ tetrahedra. These blocks alternate with the $[Sr_3Sc_2O_5]$ oxide blocks (see Fig. 1). As a result, as pointed out above, adjacent $[Fe_2As_2]$ blocks are a considerable distance apart: $L \approx 13.4$ Å. The layered structure of $Sr_3Sc_2Fe_2As_2O_5$ determines the effect[15] of anisotropic thermal lattice deformation: upon cooling the sample from 300 to 10 K, the contraction of the crystal along the *c* axis is most substantial

$$\frac{\Delta c}{c}\left(\frac{\Delta a}{a}\right)^{-1} \approx 4.2.$$

In 42226 phases, the $[Fe_2As_2]$ blocks alternate with the $[Sr_4Sc_2O_6]$ oxide blocks (see Fig. 1), which have perovskite-like structures; as a result, adjacent $[Fe_2As_2]$ blocks in 42226 phases are at a distance of $L \approx 15.5$ Å apart, *i.e.*, more remote than those in 32225 phases.

The lattice parameters of new 32225 and 42226 phases are listed in Table 2, atomic positions in these phases [by the example of $Sr_3Sc_2Fe_2As_2O_5$ (Ref. 15) and $Sr_4Sc_2O_6Fe_2As_2$ (Ref. 17)] are characterized by data summarized in Table 3.

Table 2. Lattice parameters (Å) of layered 32225 and 42226 phases and related five-component systems.

Phase	Lattice parameters		Ref.
	a	*c*	
$Sr_3Sc_2Fe_2As_2O_5$	4.069	26.876	6
$Sr_3Sc_2Fe_2As_2O_5$	4.078	26.839	15
$Sr_4Sc_2Fe_2As_2O_6$	4.045	15.802	16
$Sr_4Sc_2Fe_2As_2O_6$	4.050	15.809	17
$Sr_4Sc_2Fe_2As_2O_6$	4.048	15.804	18
$Ba_4Sc_2Fe_2As_2O_6$	4.127	16.800	24
$Sr_4(Cr_{0.8}Ti_{1.2})Fe_2As_2O_6$	3.900	15.838	19
$Sr_4(MgTi)Fe_2As_2O_6$	3.935	15.552	25
$Sr_4V_2Fe_2As_2O_6$	3.930	15.666	20
$Sr_4V_2Fe_2As_2O_6$	3.925	15.870	21
$Sr_4Cr_2Fe_2As_2O_6$	3.918	15.683	17
$Sr_4Cr_2Fe_2As_2O_6$	3.911	15.791	24
$Sr_4Sc_2Co_2As_2O_6$	4.045	15.695	16
$Sr_4Sc_2Ni_2As_2O_6$	4.087	15.405	23
$Sr_4Sc_2Fe_2P_2O_6$	4.016	15.543	22
$Sr_4Sc_2Ni_2P_2O_6$	4.044	15.231	21

Table 3. Atomic positions in structures of layered 32225 and 42226 phases and related five-component systems by the example of $Sr_3Sc_2Fe_2As_2O_5$ (Ref.15) and $Sr_4Sc_2Fe_2As_2O_6$ (Ref. 17).

Phase	$Sr_3Sc_2Fe_2As_2O_5$ (see [a])	Phase	$Sr_4Sc_2Fe_2As_2O_6$
Sr_1 (2*b*)	(0, 0, $^1/_2$)	Sr_1 (2*c*)	($-^1/_4$, $-^1/_4$, *z*); *z* = 0.1887
Sr_2 (4*e*)	(0, 0, *z*); *z* = 0.3604	Sr_2 (2*c*)	($-^1/_4$, $-^1/_4$, *z*); *z* = 0.4153
Sc (4*e*)	(0, 0, *z*); *z* = 0.0727	Sc (2*c*)	($^1/_4$, $^1/_4$, *z*); *z* = 0.3071
O_1 (8*g*)	(0, $^1/_2$, *z*); *z* = 0.0828	O_1 (4*f*)	($^1/_4$, $-^1/_4$, *z*); *z* = 0.2857
O_2 (2*a*)	(0, 0, 0)	O_2 (2*c*)	($^1/_4$, $^1/_4$, *z*); *z* = 0.4301
Fe (4*d*)	(0, $^1/_2$, $^1/_4$)	Fe (2*b*)	($^1/_4$, $-^1/_4$, 0)
As (4*e*)	(0, 0, *z*); *z* = 0.1996	As (2*c*)	($^1/_4$, $^1/_4$, *z*); *z* = 0.0854

[a] The *I*4/*mmm* space group; *Z* = 2.

Using the known [2–5] correlations between the critical temperature, lattice parameters (*a*) and the angles (α) of the As–Fe–As bonds in the $[Fe_2As_2]$ blocks for 1111 and 122 phases, these parameters were juxtaposed with those for 32225 and 42226 phases [17] (Fig. 3). It can be seen that general trends in the alteration of structural parameters for new and earlier known 1111 phases are alike. At the same time, certain differences for FeAs-phases of different stuctural groups are obvious. For example, the angles α for $Sr_4Sc_2Fe_2As_2O_6$ and CeFeAsO are very similar, whereas the parameter *a* for CeFeAsO is noticeably smaller than that for $Sr_4Sc_2Fe_2As_2O_6$. Accordingly, the correlation of bond

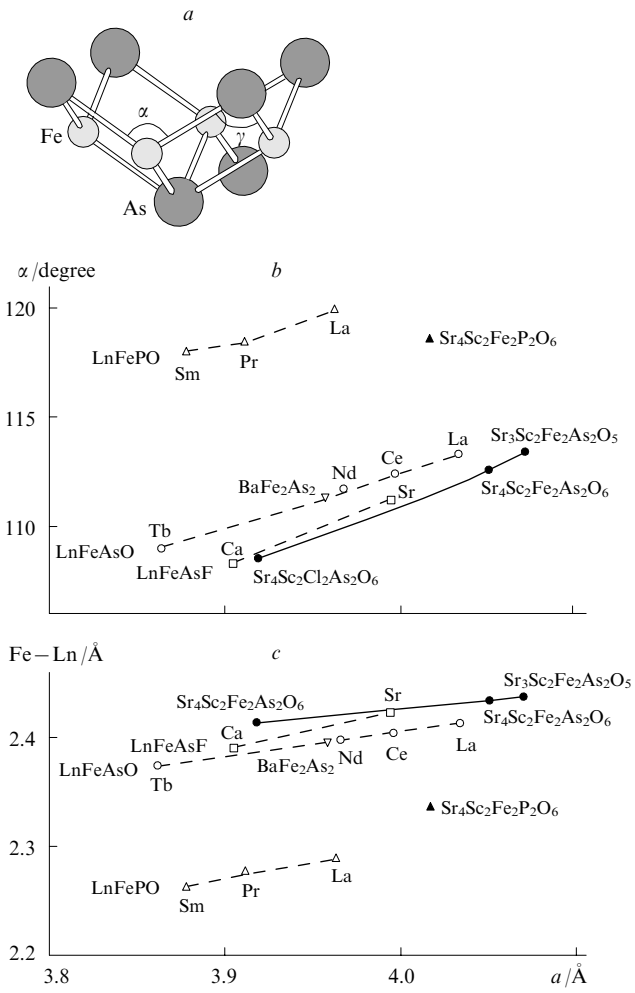


Figure 3. Variations in the As–Fe–As bond angles (*a*, *b*) and the interatomic (Fe–Ln) distances in 32225 and 42226 phases (dark dots) in comparison with some 1111 and 122 phases (light dots) depending on chemical composition.[17]

angles and lattice parameters for 32225 and 42226 phases is distinct from those for other FeAs-systems. This allows one to find new methods of the adjustment of local geometry parameters of the superconducting $[Fe_2As_2]$ layers in five-component phases.[17]

Note also that for 32225 and 42226 phases, no structural phase transitions near the boundary of superconductig areas, which is characteristic [2–5] of other FeAs-superconductors, were detected. Further research is required in order to establish details about the dependences of structural parameters of 32225 and 42226 phases on the type and concentration of dopants [25] as well as on other possible stuctural defects. The pecularities of the microstructure of samples of 32225 and 42226 phases are not studied either.

In investigating the physicochemical properties of 32225 and 42226 phases as potential materials for innovative superconductors, primary attention was given to their electrophysical and magnetic characteristics. For all the currently synthesized samples of these phases, temperature dependences of their electrical resistivity (ρ) and magnetization were measured [6, 15–25] and critical temperatures were determined based on them.

According to the available data (see Table. 1), among the currently obtained undoped 32225 and 42226 phases, $Sr_3Sc_2Fe_2As_2O_5$, $Sr_4Sc_2Fe_2As_2O_6$, $Sr_4Cr_2Fe_2As_2O_6$, $Ca_4Sc_2Fe_2As_2O_6$ and $Sr_4Sc_2Co_2As_2O_6$ have no transitions to the superconducting state, the other phases are superconductors. Among the latter, $Sr_4V_2Fe_2As_2O_6$ has the maximum $T_c \sim 37$ K (Fig. 4), and in the area of higher temperatures no distinct anomalies were observed in the temperature dependence of electrical resistivity.[20] On the contrary, no transition to the superconducting state could be revealed in a study of the dependence $\rho(T)$ for a sample of $Sr_4V_2Fe_2As_2O_6$.[21] Instead, an anomaly at ~ 175 K was registered, which was attributed to the effect of the formation of spin density waves known[2–5] for other FeAs-systems. One of the possible reasons for the divergence of results obtained in the studies cited (Refs 20 and 21) can be the effect of oxygen nonstoichiometry, which, as is known[2–5] for other oxygen-containing phases 1111 of FeAs-systems, brings about the suppression of spin fluctuations and the formation of a superconducting state. Another reason can be[20] the varying valence of vanadium ($V^{3+} - V^{4+}$).

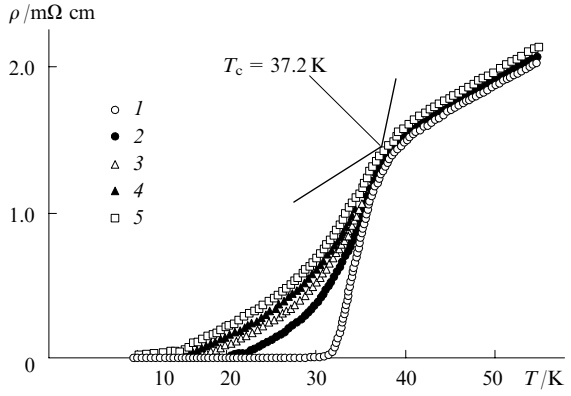


Figure 4. Temperature dependences of electrical resistivity near the onset of a critical transition ($T_c = 37.2$ K) for $Sr_4V_2Fe_2As_2O_6$ in different magnetic fields.[20]
H/T: (*1*) 0, (*2*) 1, (*3*) 3, (*4*) 6, (*5*) 9.

Quite an unexpected result was obtained for a phosphorus-containing 42226 phase, $Sr_4Sc_2Fe_2P_2O_6$: a transition to the superconducting state at $T_c^{(o)} \approx 17$ K was established.[22] It is appropriate to remind that the replacement of arsenic by phosphorus in undoped 1111 phases, which are not superconductors, also results in superconductivity, albeit the value of T_c is by far smaller ($\sim 3-5$ K).[29] Thus, the $Sr_4Sc_2Fe_2P_2O_6$ phase is currently the highest-temperature superconductor among all related phases that do not contain arsenic. Interestingly, upon substitution of nickel for iron the $Sr_4Sc_2Ni_2As_2O_6$ and $Sr_4Sc_2Ni_2P_2O_6$ phases become low-temperature superconductors with $T_c \sim 2.7$ and 3 K, respectively. In this respect, a certain analogy to 1111 phases is also observed (for LaNiPO, a transition to the superconducting state at ~ 3 K,[30] which is well described[31–34] within the framework of the standard concepts of electron-phonon mechanism in the Bardeen–Cooper–Schrieffer model, has been discovered). The general mechanism of the emergence of superconductivity in undoped 32225 and 42226 phases has no explanation so far.

The first results[18,19,25] of the study of the influence of doping on the superconductivity of new five-component phases where the above-mentioned technique of doping by partial replacement of a 3d-metal (Sc, Ti) in perovskite-like oxide blocks by atoms of other 3d-metals (Cr, Ti)[18,19] or Mg was applied,[25] seem very interesting. According to these data, for $Sr_4Cr_{0.8}Ti_{1.2}Fe_2As_2O_6$ (Ref. 19) and $Sr_4Sc_{0.8}Ti_{1.2}Fe_2As_2O_6$ (see Ref. 18) the onset of a transition to the superconducting state was observed at ~ 29.2 and 45 K, and zero resistance was at 6 and 7 K, respectively. In this case, no anomalies associated with charge density waves[17] were detected in the dependence $\rho(T)$ for $Sr_3Sc_2Fe_2As_2O_5$ (Ref. 6) and $Sr_4Sc_2Fe_2As_2O_6$. Neither are any anomalies that could provide evidence for magnetic transitions present in the temperature dependence of magnetic susceptibility $\chi(T)$ for $Sr_4Sc_2Fe_2As_2O_6$, which alters according to the Curie–Weiss type (up to 400 K),[16] whereas the dependence $\chi(T)$ for $Sr_4Sc_2Co_2As_2O_6$ (Fig. 5) points to a ferromagnetic behaviour of this phase also inherent in the LaCoAs(P)O systems with the Curie temperature of ~ 66 K.[35,36] For $Sr_4Cr_2Fe_2As_2O_6$, conversely, a transition to the antiferromagnetic state was determined.[25]

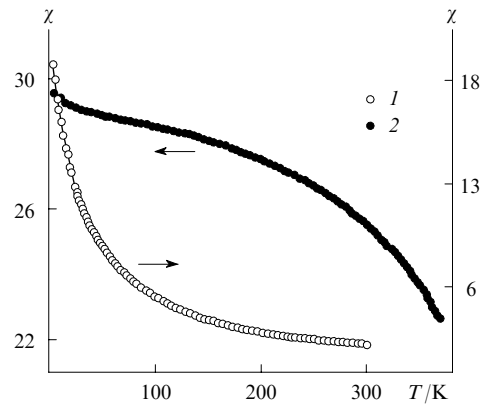


Figure 5. Temperature dependences of magnetic susceptibility (χ, in 10^{-6} emu g^{-1} Œ$^{-1}$) for $Sr_4Sc_2Fe_2As_2O_6$ (*1*) and $Sr_4Sc_2Co_2As_2O_6$ (*2*).[16]

Note that the factors that can affect the critical transition temperature to superconducting materials based on 1111, 122 and 111 phases, such as the substitution of fluorine for oxygen, the presence of vacancies in the oxygen sublattice, the replacement of alkaline-earth metal atoms by alkali or rare-earth metal atoms, have not yet been studied for the new five-component phases.

The first attempt[37] was undertaken (by the example of the $Sr_4Sc_2Fe_2P_2O_6$ and $Sr_4V_2Fe_2As_2O_6$ phases) to determine the role of pressure effect in the control of properties (first of all, the critical transition temperature) for the five-component phases involved. As evident from Fig. 6, external pressure can exert diametrically opposed effects on the superconducting transition temperature: for $Sr_4V_2Fe_2As_2O_6$, the value of $T_c^{(o)}$ increases, for $Sr_4Sc_2Fe_2P_2O_6$ this parameter decreases. The reasons for such an effect are so far obscure.

The impact of external magnetic field (H) on the transition to the superconducting state in some 42226 phases is discussed.[19,20,22,23,25] Figure 4 illustrates typical results by the example of $Sr_4V_2Fe_2As_2O_6$. It was noted that a general effect is the broadening of this transition with the

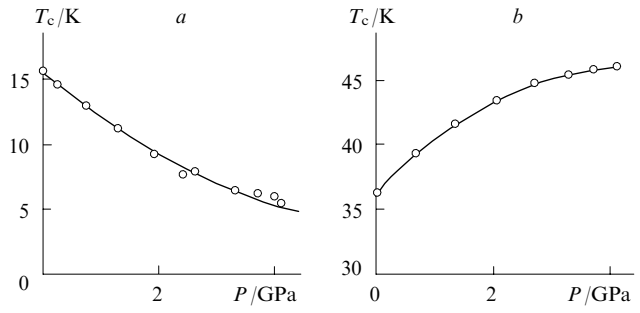


Figure 6. Variation in the critical temperature for $Sr_4Sc_2Fe_2P_2O_6$ (*a*) and $Sr_4V_2Fe_2As_2O_6$ (*b*) under the influence of external pressure.[37]

increase in H, no substantial change in $T_c^{(o)}$ values was registered except for $Sr_4Sc_2Fe_2P_2O_6$ (Ref. 22) for which the transition becomes extremely wide as H increases so that it is difficult to determine the value of $T_c^{(o)}$ (Fig. 7). The effect

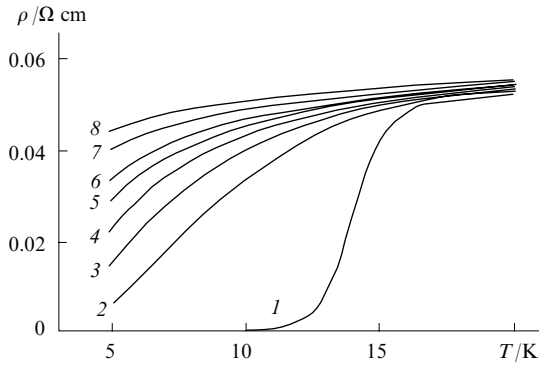


Figure 7. Temperature dependences of electrical resistivity for $Sr_4Sc_2Fe_2P_2O_6$ in different magnetic fields.[22]
H/T: (*1*) 0, (*2*) 1, (*3*) 2, (*4*) 3, (*5*) 4, (*6*) 5, (*7*) 7, (*8*) 9.

is explained[22] by porous microstructure and grain-boundary phenomena for the $Sr_4Sc_2Fe_2P_2O_6$ sample as well as by high electromagnetic anisotropy owing to the perovskite-like $[Sr_4Sc_2O_6]$ blocks that shield the conducting $[Fe_2P_2]$ blocks. Note also that for $Sr_4V_2Fe_2As_2O_6$ a sharp temperature drop in the upper critical field $H_{c2}(T)$ near $T_c^{(o)}$

$$\left(\frac{dH_{c2}}{dT}\right)_{T=T_c} \approx -11.3 \text{ T K}^{-1}$$

was registered.[20] This is considerably larger than for other FeAs-superconductors,[38–40] and according to estimates (by a formula provided in Ref. 40) for $Sr_4V_2Fe_2As_2O_6$, this gives a very high value of H_{c2} equal to $\sim$302 T.

The Hall effect was measured for samples of $Sr_3Sc_2Fe_2As_2O_5$ (Ref. 6), $Sr_4Sc_2Fe_2As_2O_6$ (Ref. 16) and $Sr_4V_2Fe_2As_2O_6$ in order to determine charge carrier types.[20] It was established that the Hall coefficient (R_H) is negative and this suggests the predomination of electron carriers in the conductivity of these systems as also in 1111 and 122 phases, whereas for 111 phases the R_H value is positive. At the same time, strong dependence of R_H on temperature[6,16] (as in the case of 1111 phases) suggests a multiband character of systems 32225 and 42226.

^{57}Fe Mössbauer (nuclear gamma-resonance) spectroscopy was used for studying $Sr_3Sc_2Fe_2As_2O_5$ (Ref. 15), $Ba_4Sc_2Fe_2As_2O_6$ and $Sr_4Cr_2Fe_2As_2O_6$ (Ref. 24). The spectrum of $Sr_3Sc_2Fe_2As_2O_5$ has a singlet shape at room temperature, upon a decrease in temperature multiplet splittings that could suggest the formation of a magnetic order are absent. Parameters of the Mössbauer spectrum of the $Sr_3Sc_2Fe_2As_2O_5$ sample (the values of isomer shift δ and quadrupole splitting ΔE_Q)[41] are in good agreement with the corresponding parameters measured on the ^{57}Fe nuclei for LaFeAsO,[42,43] LaFePO,[44] $SrFe_2As_2$,[45] and $BaFe_2As_2$.[46] Similar parameters (on the ^{57}Fe nuclei) were also obtained for $Ba_4Sc_2Fe_2As_2O_6$ and $Sr_4Cr_2Fe_2As_2O_6$, which allows one to make a conclusion about similarity in the electronic states of the $[Fe_2As_2]$ layers in these systems, at the same time the presence of antiferromagnetic ordering in chromium-containing phase 42226 was noted.[24]

IV. Simulation of the electronic structures of 32225 and 42226 phases

To date, data on the electronic stuctures of the $Sr_3Sc_2Fe_2As_2O_5$ (Ref. 47), $Sr_4Sc_2Fe_2As_2O_6$, $Sr_4Sc_2Fe_2P_2O_6$ (Ref. 48), $Ba_4Sc_2Fe_2As_2O_6$ (Ref. 24), $Sr_4Sc_2V_2As_2O_6$ (Ref. 49 and 50) phases and the titanium-doped $Sr_4Sc_2Fe_2As_2O_6$ phase (with the formal composition $Sr_4ScTiFe_2As_2O_6$) have been obtained with the aid of the computational methods of the density functional theory.[51]

For $Sr_3Sc_2Fe_2As_2O_5$, the following featues were established[47]:

— the near-Fermi bands (in the area -2 eV to $+2$ eV) of this phase [as well as for FeAs-systems 1111, 122 and 111 (Refs 2–4)] are predominantly composed of Fe3d-states with minor admixtures of As4p-states (Table 4);

— the Fermi level is located on the high-energy slope of an intense peak of a Fe3d-band near a pseudo-gap separating the bonding and antibonding Fe3d-states; therefore,

Table 4. The total $N^{tot}(E_F)$ and partial $N^l(E_F)$ densities of states at the Fermi level (states per eV), the coefficients of the low-temperature electronic heat capacity γ (mJ K^{-2} mol^{-1}) and the molar Pauli paramagnetic susceptibility (χ, in 10^{-4} emu mol^{-1}) for $Sr_3Sc_2Fe_2As_2O_5$, $Sr_4Sc_2Fe_2As_2O_6$, SrFeAsF, $BaFe_2As_2$ and LiFeAs phases.

Parameter	$Sr_3Sc_2Fe_2As_2O_5$ (Ref. 47)	$Sr_4Sc_2Fe_2As_2O_6$ (Ref. 48)	SrFeAsF (Ref. 59)	$BaFe_2As_2$ (Ref. 57)	LiFeAs (Ref. 58)
$N^{Fe3d}(E_F)$	2.918 (1.456)[a]	2.779 (1.390)[a]	1.188	1.860[a]	1.203
$N^{As}(E_F)$	0.054	0.081	0.039	0.071	0.037
$N^{tot}(E_F)$	3.579	3.754	1.540	4.553	1.527
γ	8.44	8.85	3.630	10.73	3.60
χ	1.15	1.21	0.496	1.47	0.49

[a] Calculated per iron atom.

electron or hole doping of the $Sr_3Sc_2Fe_2As_2O_5$ phase will lead to sharp changes in the density of states at the Fermi level, which has a substantial impact on the conducting and magnetic properties of this crystal;

— the Fe3d-like bands near the Fermi level are of quasi-planar character with a small dispersion $E(k)$, and upon crossing E_F form a system of electron and hole pockets;

— the Fermi surface (Fig. 8) comprises hole cylinders at the centre of the Brillouin zone (the $\Gamma-Z$ direction) and electron sheets along its edges (the A – M direction). An assumption was made [47] that the emergence mechanisms of the superconductivity of 1111, 122 and 111 phases and the new $Sr_3Sc_2Fe_2As_2O_5$ phase could be similar; this opens up prospects for further search for novel FeAs-superconductors based on both this phase and its probable homologues: $Sr_{n+1}M_nFe_2As_2O_{3n-1}$ (M = Sc, Ti, Cu, *etc.*).

Assessments [47] of the relative stability of the non-magnetic, ferromagnetic and antiferromagnetic (with a G-type spin ordering) states of $Sr_3Sc_2Fe_2As_2O_5$ demonstrated that the ferromagnetic state is transformed into non-magnetic upon self-consistency. For the antiferromagnetic phase (for which magnetic moments on the iron atoms are 0.15 μ_B), its total energy turns out to be $\sim$0.7 eV per formula unit higher than that for the non-magnetic phase. This suggests [47] properties of a paramagnetic metal for the complete (undoped) $Sr_3Sc_2Fe_2As_2O_5$ phase, which is consistent with experiment.

The electronic structures of the isoelectronic $Sr_4Sc_2Fe_2As_2O_6$ and $Sr_4Sc_2Fe_2P_2O_6$ phases (Figs 9 and 10) prove [48] to be quite alike. The Fermi surfaces of these phases are also of quasi-two-dimensional character and comprise hole cylinders in the centre of the Brillouin zone (the $\Gamma-Z$ direction) and electron sheets along its edges (see Fig. 9). By the example of these phases consider the distribution of density of electronic states (DOS) in more detail. A group of low-energy bands (band *A* of density of states, Fig. 10) located in the energy range -12 to -10 eV below E_F is basically composed of the As4s-(P3s)-states. The group of occupied bands that is next in energy (*B*) is situated in the interval -6 to -2 eV and is separated from the near-Fermi bands (band *C*) by a pseudo-gap.

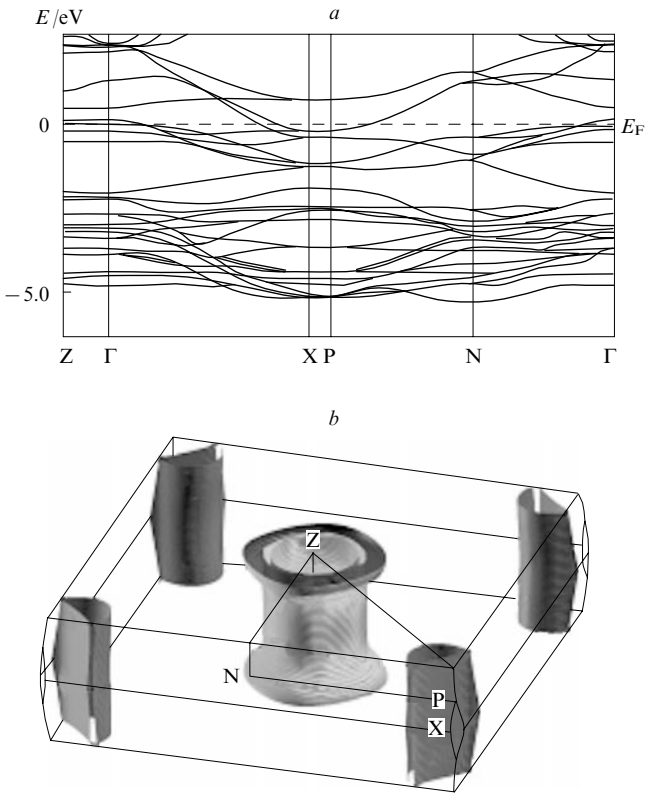


Figure 8. Energy bands near the Fermi level (*a*) and the Fermi surface (*b*) for $Sr_3Sc_2Fe_2As_2O_5$.[47]

This band has a mixed composition involving the Fe3d, As4p- (P3p), Sc3d, and O2p states. Given the distributions of the corresponding atoms between the $[Sr_4Sc_2O_6]$ and $[Fe_2(As,P)_2]$ blocks these states are responsible for the formation of the covalent bonds Fe – As(P) {in the $[Fe_2(As,P)_2]$ blocks} and Sc – O (in the $[Sr_3Sc_2O_5]$ blocks) resulting from the hybridization of the Fe3d – As4p- (P3p) and Sc3d – O2p states, respectively.

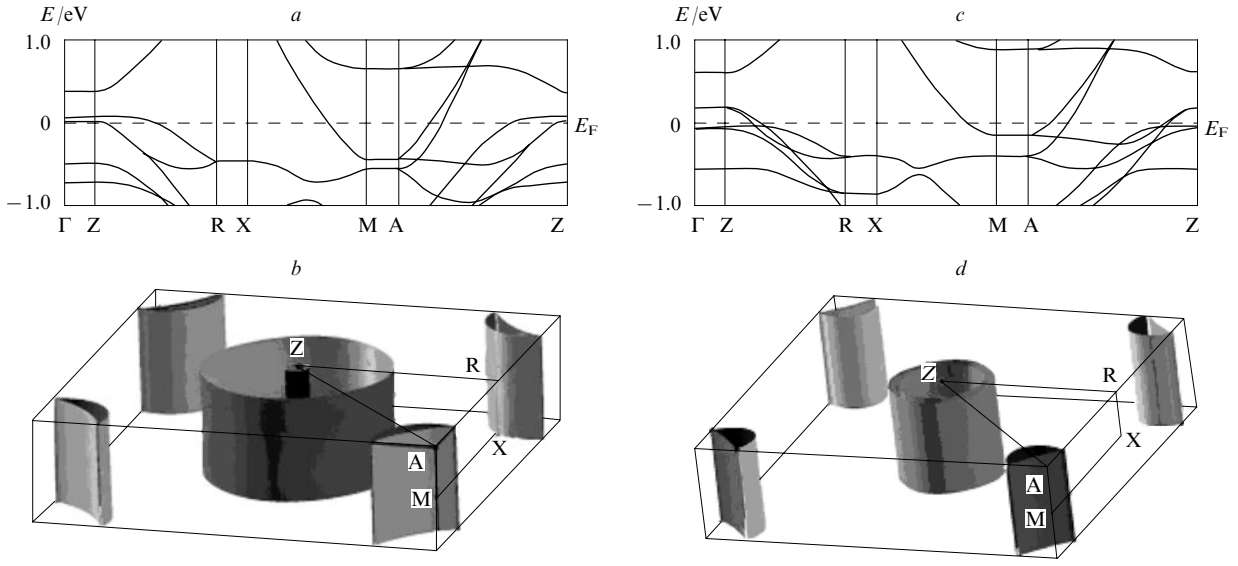


Figure 9. Energy bands near the Fermi level (*a*, *c*) and the Fermi surfaces (*b*, *d*) for $Sr_4Sc_2Fe_2P_2O_6$ (*a*, *b*) and $Sr_4Sc_2Fe_2As_2O_6$ (*c*, *d*).[48]

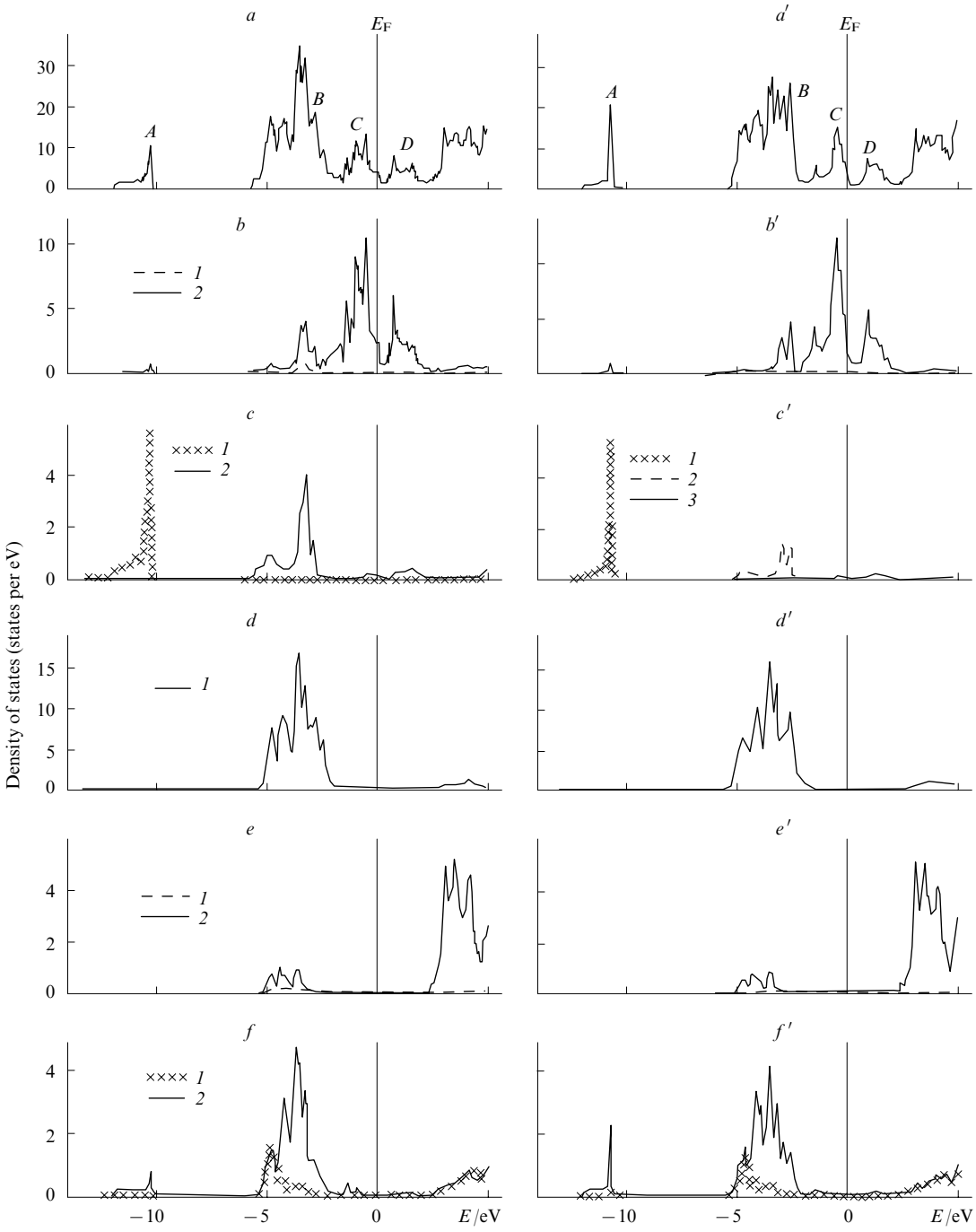


Figure 10. The total (a, a') and partial (b–f, b'–f') densities of electronic states for $Sr_4Sc_2Fe_2P_2O_6$ (left) and $Sr_4Sc_2Fe_2As_2O_6$ (right).[48] (b, b'): (*1*) Fe4p, (*2*) Fe3d; (c): (*1*) P3s, (*2*) P3p; (c'): (*1*) As4s, (*2*) As4p; (d, d'): (*1*) O2p; (e, e'): (*1*) Sc4p, (*2*) Sc3d; (f, f'): (*1*) Sr5s, (*2*) Sr5p.

It is essential that the near Fermi band *C* of scandium-containing 42226 phases is made up exclusively of the $[Fe_2(As,P)_2]$ block states, which will make a determining contribution to the conductivity of these systems. On the contrary, the valence states of the positively charged $[Sr_4Sc_2O_6]$ blocks (charge reservoir layers) are virtually not involved in the formation of the near Fermi bands. Accordingly, the $Sr_4Sc_2Fe_2As_2O_6$ and $Sr_4Sc_2Fe_2P_2O_6$ phases can be described [48] as systems composed of the conducting $[Fe_2(As,P)_2]$ blocks that alternate with the insulating $[Sr_4Sc_2O_6]$ blocks.

As demonstrated by calculations,[24, 48–51] the electronic structure of 42226 phases is crucially dependent on the transition metal atom type in the $[Sr_4M_2O_6]$ blocks. Thus, even partial substitution of titanium for scandium in $Sr_4Sc_2Fe_2As_2O_6$ gives rise [51] to alterations in the properties of the blocks: $[Sr_4Sc_2O_6]$ behaves as an insulator and $[Sr_4ScTiO_6]$ behaves as a metal while the system remains non-magnetic overall. Yet sharper changes come about (Fig. 11) upon the introduction of vanadium in the oxide blocks:[49] the system turns magnetic, and the $[Sr_4V_2O_6]$ blocks adopt a spin configuration that is characteristic of semi-metallic magnets.[52] As is known,[53, 54] such systems are

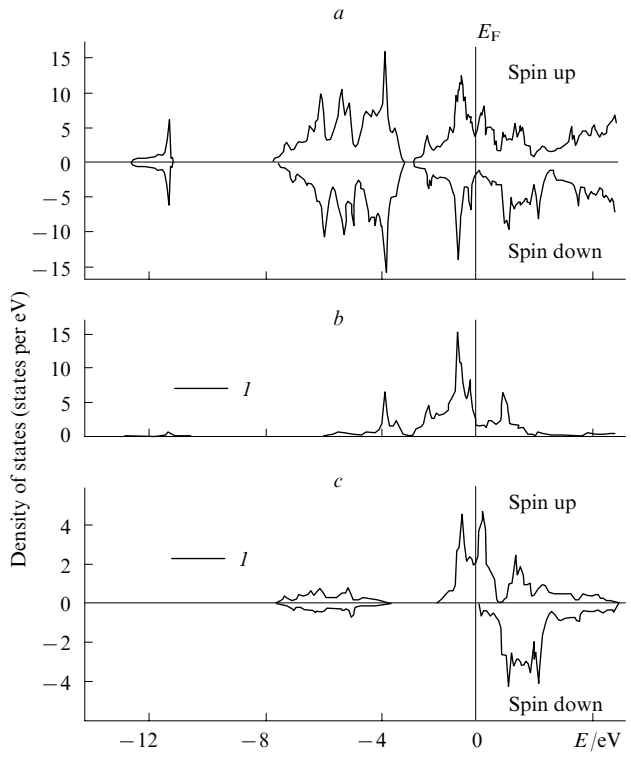


Figure 11. The total (*a*) and partial densities (*b*, *c*) of the spin states of the Fe and V atoms for $Sr_4V_2Fe_2As_2O_6$.[49]
(*b*): (*1*) Fe3d; (*c*): (*1*) V3d.

charaterized by a non-zero density of charge carriers at the Fermi level for one direction of a spin projection $[(N\uparrow(E_F) > 0]$, but contain a forbidden gap for the opposite direction of the spin projection $[N\downarrow(E_F) = 0]$. Hence in the ideal case for semi-metallic magnets the polarization of spin density (P) at the Fermi level is

$$P = \frac{N\uparrow(E_F) - N\downarrow(E_F)}{N\uparrow(E_F) + N\downarrow(E_F)} = 1.$$

As a result, the conductivity of semi-metallic magnets occurs through dedicated spin channels for which different types of magnetic structure can be realized: ferro-, antiferro- and ferrimagnetic.

Thus, according to calculations,[24, 48–51] a unique series of layered FeAs-materials forms in phases 42226 depending on the type of the transition metal M in the $[Sr_4M_2O_6]$ blocks. Thus $Sr_4Sc_2Fe_2As_2O_6$ is composed of the alternating non-magnetic metallic $[Fe_2As_2]$ and insulating $[Sr_4Sc_2O_6]$ blocks, for the hypothetical $Sr_4Ti_2Fe_2As_2O_6$ phase the alternating non-magnetic $[Fe_2As_2]/[Sr_4Ti_2O_6]$ blocks are of the metallic conductivity type, $Sr_4V_2Fe_2As_2O_6$ is made up of the packed metallic non-magnetic $[Fe_2As_2]$ blocks and the $[Sr_4V_2O_6]$ blocks of the semi-metallic magnet type, and finally, the $[Sr_4Cr_2O_6]$ blocks for $Sr_4Cr_2Fe_2As_2O_6$ are of the magnetic metal type.

In conclusion, let us examine some features of interatomic interactions in 32225 and 42226 phases.[47–51] Given the formal valence of the component atoms and their distribution between structural blocks, the ionic formula $Sr_3Sc_2Fe_2As_2O_5$ can be represented as $([Sr^{2+}]_3[Sc^{3+}]_2[O^{2-}]_5)^{2+}([Fe^{2+}]_2[As^{3-}]_2)^{2-}$. Analogously, the formal charge state of elements in blocks for 42226 phases can be represented as $([Sr^{2+}]_4[M^{3+}]_2[O^{2-}]_6)^{2+}.([Fe^{2+}]_2[As^{3-}]_2)^{2-}$. In other words, charge transfer between blocks in $Sr_3Sc_2Fe_2As_2O_5$ takes place

$$[Sr_3Sc_2O_5]^{2+} \longrightarrow [Fe_2As_2]^{2-},$$

the $[Sr_3Sc_2O_5]$ blocks playing the role of charge reservoirs as in the case 42226, 1111, 122 and 111 phases.[55–62] Consequently, ionic bonds emerge between both atoms of different sorts in each block and neighbouring blocks. Numerical calculations for $Sr_3Sc_2Fe_2As_2O_5$ (within the framework of the Bader[63] scheme) permitted the evaluation[47] of the effective charges (Q) of atoms and individual blocks. In particular, inter-layer charge transfer between the blocks $\Delta Q([Sr_3Sc_2O_5] \rightarrow [Fe_2As_2])$ is much smaller than the value inferred from estimates based on formal atomic valences and equal to ~ 0.31 e, which is close to the analogous calculated values of ΔQ for other FeAs-superconductors (Table 5).

However, the mentioned ionic and metallic bonds (Fe–Fe, inside the $[Fe_2As_2]$ layers resulting from the delocalized Fe3d-states in the near Fermi area) for

Table 5. Molecular layer charges (e) for $Sr_3Sc_2Fe_2As_2O_5$,[47] calculated within the framework of the Bader scheme, in comparison with analogous values for SrFeAsF and LaFeAsO.[59]

$Sr_3Sc_2Fe_2As_2O_5$	LaFeAsO	SrFeAsF
+0.534/+0.415 (Sr);[a]	1.115 (La);	+0.465 (Sr);
+1.754 (Fe);	1.772 (Fe);	+1.741 (Fe);
−2.055 (As);	−2.113 (As);	−2.050 (As);
+1.071 (Sc);	−0.724 (O)	−0.157 (F)
−0.612/−0.603 (O)[a]		
+0.301 $[Sr_3Sc_2O_5]$	+0.391 [LaO]	+0.280 [SrF]
−0.301 $[Fe_2As_2]$	−0.391 $[Fe_2As_2]$	−0.280 $[Fe_2As_2]$

[a] For structurally nonequivalent atoms.

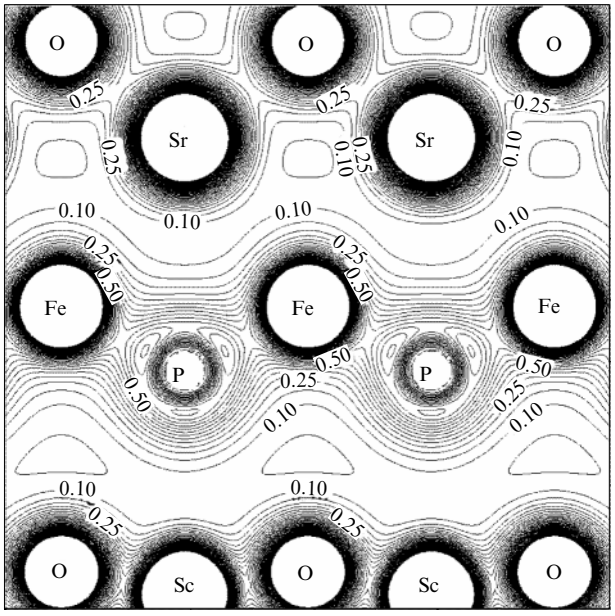


Figure 12. Charge density distribution (e Å^3) for $Sr_4Sc_2Fe_2P_2O_6$ in the plane of section (100).[48]

$Sr_3Sc_2Fe_2As_2O_5$ and 1111, 122 and 111 phases prove similar, whereas the system of covalent bonds has a number of distinctions: the covalent Sc–O bonds are formed inside the $[Sr_3Sc_2O_5]$ layers (due to the hybridization of the Sc3d–O2p states) and the inter-layer $[Fe_2As_2]/[Fe_2As_2]$ As–As bonds characteristic of a number of other FeAs-superconductors [62] are absent due to significant spacing between these blocks in the structure of $Sr_3Sc_2Fe_2As_2O_5$.

Thus, based on calculations [47–51] one can conlcude that 32225 and 42226 phases have a complex system of anisotropic interatomic bonds, *viz*., mixed covalent-ionic-metallic bonds are produced inside $[Fe_2As_2]$ and oxide blocks. These blocks are bound to one another predominantly by ionic interactions, which is clearly evident, for example, on the charge density map for $Sr_4Sc_2Fe_2P_2O_6$ (Fig. 12). Taking into consideration the above discussion, 32225 and 42226 phases can be described as ionic metals.

V. Conclusion

Let us indicate the following results of investigations into a new family of superconductors discovered in 2009, *viz*., layered five-component oxypnictides of transition metals, as the first ones.

Along with apparent elements of similarity of 32225 and 42226 phases with the FeAs-superconductors known earlier (layered crystal structure including the $[Fe_2As_2]$ conducting blocks, sharply anisotropic conductivity type and some others [2–5]), representatives of the family of the new five-component phases manifest some important features:

— they do not contain alkali or f-metal atoms;

— the conducting $[Fe_2As_2]$ blocks are at extremely large distances from each other, $\sim$13.4 to 15.5 Å;

— transition to the superconducting state can be reached as a result of partial replacement of transition metal atoms in oxide blocks by atoms of other transition or alkaline-earth metals;

— for a number of 42226 phases, the superconductivity without doping has been revealed; in such phases, there are no prerequisites for the emergence of superconductivity known for conventional FeAs-superconductors: antiferromagnetic order and phase structural transitions;

— for $Sr_4Sc_2Fe_2P_2O_6$, a critical temperature of $T_c \approx 17$ K was registered; this is currently maximum for all the known phosphorus-containing analogues of FeAs-superconductors, while $Sr_4V_2Fe_2As_2O_6$ has $T_c \approx 37$ K, which is also a record value among all the known undoped FeAs-systems;

— unlike 1111, 122 and 111 phases, which have a common type of the electronic stucture of structural blocks (the metal-like $[Fe_2As_2]$ layers alternating with charge reservoir blocks of the insulator type), five-component 42226 phases represent a variety of hybrid electronic structures of the $[Sr_4M_2O_6]/[Fe_2As_2]$ blocks. Depending on the type of the transition metal M, these hybrids can be represented by an insulator/metal ($Sr_4Sc_2Fe_2As_2O_6$), metal/metal ($Sr_4Ti_2Fe_2As_2O_6$), magnetic semi-metal/metal ($Sr_4V_2Fe_2As_2O_6$) or magnetic metal/metal ($Sr_4Cr_2Fe_2As_2O_6$) structures. Presumably, such hybrid structures can also be formed in the family of related 32225 phases.

The indicated distinctions of the properties of 32225 and 42226 phases from those of the earlier-known FeAs-superconductors, undoubtedly, will be essential in further development of concepts of superconductivity mechanisms in iron-containing materials. Besides, much richer chemical composition of the structural blocks of 32225 and 42226 phases (containing, particularly, transition metals that can manifest varying valence) opens up a plethora of methods for fine tuning of their properties, which will attract of researchers attention to this new group of systems.

In conclusion, resting on the experience of the previous studies of FeAs-superconductors,[2–5] one can point out directions of the nearest investigations into this interesting family of materials. In the area of synthesis, one of the major objectives seems to be the development of the preparation methods of single-crystalline samples for exploring the anisotropy of physical properties. Apart from it, systematic studies on the preparation of samples doped in different sublattices (the $[Sr_4M_2O_6]$ ($[Sr_3M_2O_5]$)/$[Fe_2As_2]$ blocks) as well as samples with a controlled oxygen non-stoichiometry are required. This will enable a detailed examination of the role of electron and (or) hole doping.

Of greatest interest is the exploration of details of structural and magnetic charateristics in correlation with superconducting parameters. The pressure effect on the properties of five-component oxypnictides is little studied. The elucidation of the role of electronic correlations in the formation of subtle features of the electronic and magnetic characteristics of these phases belongs to the issues of paramount importance.

Undoubtedly, the vast experience in the research of related FeAs-superconductors, which has been acquired over the last period, gives cause to expect a succesful resolution of the indicated problems.

This work was carried out with financial support from the Russian Foundation for Basic Research (Project No. 09-03-00946). The author thanks PhD I R Shein (Physics and Mathematics), who co-authored the research works on the electronic structures of the new phases, for useful discussions.

References

1. Y Kamihara, T Watanabe, M Hirano, H Hosono *J. Am. Chem. Soc.* **130** 3296 (2008)
2. M V Sadovskii *Usp. Fiz. Nauk* **178** 1243 (2008) [*Physics-Uspekhi* **51** 1201 (2008)]
3. A L Ivanovskii *Usp. Fiz. Nauk* **178** 1272 (2008) [*Physics-Uspekhi* **51** 1229 (2008)]
4. Yu A Izyumov, E Z Kurmaev *Usp. Fiz. Nauk* **178** 1307 (2008) [*Physics-Uspekhi* **51** 1261 (2008)]
5. Yu A Izyumov, E Z Kurmaev *Vysokotemperaturnye Sverkhprovodniki na Osnove FeAs-Soedinenii* (High-Temperature Superconductors Based on FeAs-Compounds) (Moscow, Izhevsk: NITs 'Regulyarnaya i Khaoticheskaya Dinamika', 2009)
6. X Zhu, F Han, G Mu, B Zeng, P Cheng, B Shen, H H Wen *Phys. Rev. B* **79** 024516 (2009)
7. Z Ren, W Lu, J Yang, W Yi, X L Shen, Z C Li, G C Che, X L Dong, L L Sun, F Zhou, Z X Zhao *Chin. Phys. Lett.* **25** 2215 (2008)
8. C Wang, L Li, S Chi, Z Zhu, Z Ren, Y Li, Y Wang, X Lin, Y Luo, S Jiang, X Xu, G Cao, Z Xu *Europhys. Lett.* **83** 67006 (2008)
9. M Rotter, M Tegel, D Johrendt, I Schellenberg, R Poettgen *Phys. Rev. B* **78** 020503R (2008)
10. M Rotter, M Tegel, D Johrendt *Phys. Rev. Lett.* **101** 107006 (2008)
11. K Sasmal, B Lv, B Lorenz, A M Guloy, F Chen, Y Y Xue, C W Chu *Phys. Rev. Lett.* **101** 107007 (2008)
12. X C Wang, Q Q Liu, Y X Lv, W B Gao, L X Yang, R C Yu, F Y Li, C Q Jin *Solid State Commun.* **148** 538 (2008)

13. J H Tapp, B Lv, K Sasmal, B Lorenz, P C W Cu, A M Guloy *Phys. Rev. B* **78** 060505R (2008)
14. J C Hsu, J Y Luo, K W Yeh, T K Chen, T W Huang, P M Wu, Y C Lee, Y L Huang, Y Y Chu, D C Yan *Proc. Natl. Acad. Sci. USA* **105** 14262 (2008)
15. M Tegel, I Schellenberg, F Hummel, R Pöttgen, D Johrendt *Z. Naturforsh., A* **64** 815 (2009)
16. Y L Xie, R H Liu, T Wu, G Wu, Y A Song, D Tan, X F Wang, H Chen, J J Ying, Y J Yan, Q J Li, X H Chen *Europhys. Lett.* **86** 57007 (2009)
17. H Ogino, Y Katsura, S Horii, K Kishio, J Shimoyama *Supercond. Sci. Technol.* **22** 085001 (2009)
18. G F Chen, T L Xia, H X Yang, J Q Li, P Zheng, J L Luo, N L Wang *Supercond. Sci. Technol.* **22** 072001 (2009)
19. X Zhu, F Han, G Mu, P Cheng, B Shen, B Zeng, H H Wen *Sci. China, Ser. G* **52** 1876 (2009)
20. X Zhu, F Han, G Mu, P Cheng, B Shen, B Zeng, H H Wen *Phys. Rev. B* **79** 220512R (2009)
21. A Pal, A Vajpayee, R S Meena, H Kishan, V P S Awana *J. Supercond. Novel Magnet.* **22** 619 (2009)
22. H Ogino, Y Matsumura, Y Katsura, K Ushiyama, S Horii, K Kishio, J Shimoyama *Supercond. Sci. Technol.* **22** 075008 (2009)
23. Y Matsumura, H Ogino, S Horii, Y Katsura, K Kishio, J Shimoyama *Appl. Phys. Express* **2** 063007 (2009)
24. M Tegel, F Hummel, S Lackner, I Schellenberg, R Plttgen, D Johrendt *Z. Anorg. Allg. Chem.* **635** 2242 (2009)
25. S Sato, H Ogino, N Kawaguchi, Y Katsura, K Kishio, J Shimoyama arXiv:cond-mat/0909.2945 (2009)
26. E Makovicky, Z Johan, S Kapur-Moller *Neues Jahrb. Mineral. Abh.* **138** 122 (1980)
27. W J Zhu, P H Hor *J. Solid State Chem.* **134** 128 (1997)
28. W J Zhu, P H Hor *Inorg. Chem.* **36** 3576 (1997)
29. R E Baumbach, J J Hamlin, L Shu, D A Zocco, N M Crisosto, M B Maple *New J. Phys.* **11** 025018 (2009)
30. M Tegel, D Bichler, D Johrendt *Solid State Sci.* **10** 193 (2008)
31. S Lebègue *Phys. Rev. B* **75** 35110 (2007)
32. Y Kamihara, M Hirano, H Yanagi, T Kamiya, Y Saitoh, E Ikenaga, K Kobayashi, H Hosono *Phys. Rev. B* **77** 214515 (2008)
33. W B Zhang, X B Xiao, W Y Yu, N Wang, B Y Tang *Phys. Rev. B* **77** 214513 (2008)
34. A Subedi, D J Singh, M H Du *Phys. Rev. B* **78** 060506 (2008)
35. H Yanagi, R Kawamura, T Kamiya, Y Kamihara, M Hirano, T Nakamura, H Osawa, H Hosono *Phys. Rev. B* **77** 224431 (2008)
36. A S Sefat, M A McGuire, R Jin, B C Sales, D Mandrus, L M D Cranswick, P W Stephens, K H Stone *Phys. Rev. B* **78** 104505 (2008)
37. H Kotegawa, T Kawazoe, H Tou, K Murata, H Ogino, K Kishio, J Shimoyama *J. Phys. Soc. Jpn.* **78** 083702 (2009)
38. X Zhu, H Yang, L Fang, G Mu, H H Wen *Supercond. Sci. Technol.* **21** 105001 (2008)
39. G Mu, B Zeng, X Zhu, F Han, P Cheng, B Shen, H H Wen *Phys. Rev. B* **79** 104501 (2009)
40. Z Wang, H Q Luo, C Ren, H H Wen *Phys. Rev. B* **78** 140501R (2008)
41. N R Werthamer, E Helfand, P Hohenberg *Phys. Rev. Lett.* **147** 295 (1966)
42. S Kitao, Y Kobayashi, S Higashitaniguchi, M Saito, Y Kamihara, M Hirano, T Mitsui, H Hosono, M Seto *J. Phys. Soc. Jpn.* **77** 103706 (2008)
43. H H Klauss, H H Luetkens, R Klingeler, C Hess, F J Litterst, M Kraken, M M Korshunov, I Eremin, S L Drechsler, R Khasanov, A Amato, J Hamann-Borrero, N Leps, A Kondrat, G Behr, J Werner, B Buchner *Phys. Rev. Lett.* **101** 077005 (2008)
44. M Tegel, I Schellenberg, R Poettgen, D Johrendt *Z. Naturforsch., B* **63** 1057 (2008)
45. M Tegel, M Rotter, V Weiss, F Schappacher, R Poettgen, D Johrendt *J. Phys.: Condens. Matter* **20** 452201 (2008)
46. M Rotter, M Tegel, D Johrendt, I Schellenberg, W Hermes, R Poettgen *Phys. Rev. B* **78** 020503 (2008)
47. I R Shein, A L Ivanovskii *Pis'ma Zh. Eksp. Teor. Fiz.* **89** 40 (2009) [a]
48. I R Shein, A L Ivanovskii *Phys. Rev. B* **79** 245115 (2009)
49. I R Shein, A L Ivanovskii *J. Supercond. Novel Maget.* **22** 613 (2009)
50. K W Lee, W E Pickett *Phys. Rev.* **80** 144522 (2009)
51. I R Shein, A L Ivanovskii *Central Eur. J. Phys.* (2010); DOI:10.247/s11534-009-0120-y (2009)
52. R A De Groot, F M Mueller, P G Vanengen, H J Buschov *Phys. Rev. Lett.* **50** 2024 (1983)
53. V Yu Irkhin, M I Katsnel'son *Usp. Fiz. Nauk* **164** 705 (1994) [*Physics-Uspekhi* **37** 659 (1994)]
54. A L Ivanovskii *Usp. Fiz. Nauk* **177** 1087 (2007) [*Physics-Uspekhi* **50** 1031 (2007)]
55. I R Shein, A L Ivanovskii *Scr. Mater.* **59** 1099 (2008)
56. I R Shein, V L Kozhevnikov, A L Ivanovskii *Phys. Rev. B* **78** 104519 (2008)
57. I R Shein, A L Ivanovskii *Pis'ma Zh. Eksp. Teor. Fiz.* **88** 115 (2008) [a]
58. I R Shein, A L Ivanovskii *Pis'ma Zh. Eksp. Teor. Fiz.* **88** 378 (2008) [a]
59. I R Shein, A L Ivanovskii *Pis'ma Zh. Eksp. Teor. Fiz.* **88** 781 (2008) [a]
60. I R Shein, A L Ivanovskii *Physica C* **469** 15 (2009)
61. I R Shein, A L Ivanovskii *Phys. Rev. B* **79** 054510 (2009)
62. I R Shein, A L Ivanovskii *Zh. Strukt. Khim.* **50** 540 (2009) [b]
63. R F W Bader *Atoms in Molecules: A Quantum Theory, International Series of Monographs on Chemistry* (Oxford: Clarendon Press, 1990)

[a] — *J. Exp. Theor. Phys. Lett. (Engl. Transl.)*
[b] — *J. Struct. Chem. (Engl. Transl.)*